Analysis of localization transitions using nonparametric unsupervised learning

Carlo Vanoni[1,2,*] and Vittorio Vitale[3,†]
[1]*SISSA, International School for Advanced Studies, via Bonomea 265, 34136 Trieste, Italy*
[2]*INFN Sezione di Trieste, Via Valerio 2, 34127 Trieste, Italy*
[3]*Université Grenoble Alpes, CNRS, LPMMC, 38000 Grenoble, France*

(Received 4 December 2023; revised 28 June 2024; accepted 1 July 2024; published 12 July 2024)

We propose a new viewpoint on the study of localization transitions in disordered quantum systems, showing how critical properties can be seen also as a geometric transition in the data space generated by the classically encoded configurations of the disordered quantum system. We showcase our approach to the Anderson model on regular random graphs, known for displaying features of interacting systems, despite being a single-particle problem. We estimate the transition point and verify the critical exponents in agreement with the best-known results in the literature. We provide a simple and coherent explanation of our findings, discussing the applicability of the method in real-world scenarios with a modest number of measurements.

DOI: 10.1103/PhysRevB.110.024204

I. INTRODUCTION

In the last decades, a huge effort has been devoted to understanding nonequilibrium phases of matter, which circumvent the maximum-entropy constraint of thermal equilibrium [1,2]. Within this class of problems, the complete characterization of the breakdown of ergodicity induced by disorder in quantum systems represents one of the standing open quests [3]. Together with the huge theoretical effort, there has been increasingly large attention to these unusual phases of matter also in the experimental community; as a consequence of the possibility of realizing theoretical models in the laboratory [4–9]. However, it is often difficult to find observables that are readily accessible and theoretically predictable.

In this work, we propose a data-science-inspired method in the context of disordered quantum systems, and, in particular, we show that localization transitions can also be investigated through the behavior of the classically encoded configurations in data space. To this end, we employ principal components analysis (PCA), which is used to detect the most relevant directions in data space and to compress (to project) the data set toward the significant and restricted manifold [10,11]. From the eigendecomposition of the sample covariance matrix, we introduce the Rényi-entropy of the normalized eigenvalues λ_j's ($\sum_{j=1}^{d}\lambda_j = 1$) as

$$S_{\mathrm{PCA}}^{(n)} := \frac{1}{1-n}\ln\sum_{j=1}^{d}\lambda_j^n, \tag{1}$$

and we show analytically that S_{PCA}, i.e., $S_{\mathrm{PCA}}^{(n=1)}$, is linked to the participation entropy, often employed for investigating disordered induced transitions [12–14]. Therefore, unlike the usual nonparametric approaches, our physically informed method is guaranteed to work, in the limit of sufficiently large samples. We show that the infinite-order $S_{\mathrm{PCA}}^{\infty}$ can be employed to estimate the critical point with remarkable accuracy in agreement with recent results [12,15] and displays universal behavior around the transition. Moreover, we employ a data set whose dimension is smaller than the full Hilbert space, thus being readily applicable in modern quantum simulators where large data sets of snapshots of the state of the system are routinely collected [16–19].

We remark here that data-science-inspired approaches have already found several successful applications in various fields, ranging from classical and quantum statistical physics [20–31] to molecular science and quantum chemistry [32,33].

To prove the validity of our approach, we showcase it on a prototypical example of disordered quantum systems displaying a localization transition: the Anderson model on random regular graphs (RRGs). These graphs display Anderson localization [34] with an usual scaling of expectation values with system size [12,13,35–41], andare especially hard to tackle numerically [12,42], thus being the ideal test bench for the method we propose. In the Supplemental Material [43] we provide more details on S_{PCA} and our analysis, and present results for a many-body disordered model that is believed to display a localization transition, showing that the method presented in this work is effective also for interacting systems.

The remainder of the work is structured as follows. In Sec. II we present the method we use to sample the wave function and the rationale behind the analysis of the data. In Sec. III we exploit the Anderson model on RRGs, giving a quick presentation of the system and its properties, and showcasing the effectiveness of the approach. Finally, in Sec. IV we give our conclusions and discuss possible outlooks.

II. WAVE FUNCTION SAMPLING AND ANALYSIS

The interest in nonparametric unsupervised learning methods relies on their vast range of applicability, a consequence

*Contact author: cvanoni@sissa.it
†Contact author: vittorio.vitale@lpmmc.cnrs.fr

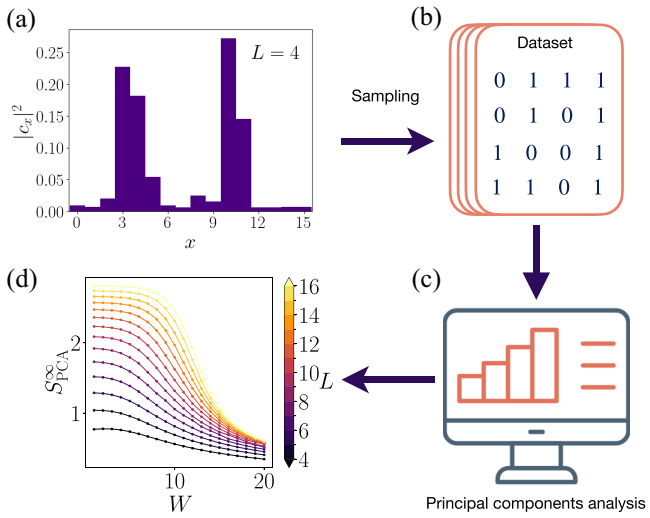

FIG. 1. Sketch of the approach used in this work. Given a quantum state $|\psi\rangle$, (a) we chose a basis $|\psi_x\rangle$ and we sample (measure) the state according to the probability distribution $|c_x|^2 = |\langle\psi_x|\psi\rangle|^2$. In this example, we consider a system with Hilbert space dimension equal to 2^L ($L = 4$). (b) We encode the measurement outcome as a string of zeros and ones corresponding to the binary representation of the integer $x \in [0, 2^L]$, labeling the basis state. (c) We perform the principal components analysis (PCA) and extract the information we are interested in by averaging over several realizations of the disorder. In (d), we show the behavior of $S^{\infty}_{\rm PCA} = -\ln\lambda_1$ [see Eq. (1) and text for details] as a function of the disorder strength W, for several sizes L.

of their agnosticism towards the problem under analysis. Such versatility is ensured by the fact that the only required input is a data set, which, in principle, can come from any sort of source, and whose geometrical properties are analyzed to extract information from the underlying physical system. In our case, the data sets consist of matrices in which each row corresponds to a single snapshot of a wave function, i.e., a measurement in a given basis [see Fig. 1(b)]. However, the method presented here may be applied to a plethora of experimental and numerical situations.

In practice, let us assume to have a state described by

$$|\psi\rangle = \sum_{x=1}^{\mathcal{N}} c_x\,|\psi_x\rangle\,, \tag{2}$$

where $\{|\psi_x\rangle\}_{x=1,\ldots,\mathcal{N}}$ is a suitable basis in the Hilbert space $\mathcal{H}$ of dimension $\mathcal{N} = \dim(\mathcal{H})$. The sampling of $|\psi\rangle$ amounts to sample, according to the probabilities $|c_x|^2$, the corresponding basis vectors $|\psi_x\rangle$. The choice of the relevant basis and the encoding of the sampling into an actual data set is one of the aspects to be investigated. For example, considering a chain of qubits, one could measure a state $|\psi\rangle$ in the computational basis and getting as an outcome a string of zeros and ones. In this work, we label as $X_i = (n_{i,1}, \ldots, n_{i,d})$ an element of the configuration space, where each $n_{i,x}$, called "feature," encodes some information of the sampled state; e.g., in the previous scenario, each feature corresponds to the measured state of the qubit (say 0 or 1) and the total number of features d is equal to the size of the system. The full target data set is a collection of N_r repetitions of X_i:

$$X = (X_1, X_2, \ldots, X_{N_r})^T \tag{3}$$

and can be represented as a $(N_r \times d)$ matrix $X_{i,j}$.

Concretely, the method we employ is the following. We define the centered data set X_c, whose elements are

$$(X_c)_{i,j} = X_{i,j} - \frac{1}{N_r}\sum_i X_{i,j} \tag{4}$$

and compute the covariance matrix $C = X_c^T X_c/(N_r - 1)$. Then, we perform the eigendecomposition $C = V^T K V$, where $K = \mathrm{diag}(k_1, \ldots, k_r)$ is the diagonal matrix of the r eigenvalues of C ordered in descending order, and $V = (v_1, \ldots, v_r)$ is the rotation whose columns v_j identify the jth relevant directions. In the new reference frame defined by V, the variance of the data along the jth direction is given by k_j, and thus $\lambda_j \equiv k_j/(\sum_i k_i)$ represents the percentage of encoded information along the direction v_j and is dubbed the jth *explained variance ratio* ($\lambda_1 > \lambda_2 > \ldots > \lambda_r$).

The motivation for our study comes from the understanding that the $S_{\rm PCA}$ — recently introduced as a measure of the information content of a physical data set [25,27] — is connected to the participation entropy. This is particularly relevant since the participation entropy is the typical quantity of interest when studying disordered systems and is used for estimating an order parameter: the fractal dimension [12,13,37,44–46]. The presence of such a connection between $S_{\rm PCA}$ and participation entropy is intriguing as, in the usual scenarios when nonparametric estimators are employed, a clear physical picture is missing. Here we show that studying the principal components is physically meaningful as they are connected to an order parameter and thus they are guaranteed to store information of the physical process.

Let us link $S_{\rm PCA}$ and participation entropy by considering the sampling of a state written as in Eq. (2). For each sample on the basis $\{|\psi_x\rangle\}_{x=1,\ldots,\mathcal{N}}$, we obtain as an outcome an integer x with probability $|c_x|^2$. Let us assume to encode this as an $\mathcal{N}$-dimensional vector with only a nonzero entry corresponding to the index x of the sampled basis vector $|\psi_x\rangle$. Then, the element of the configuration space would be vectors of the type $X_i = (0, \ldots, 0, 1, 0, \ldots, 0)$. In Ref. [43], we proved that for a large enough number of samplings $N_r \gg \mathcal{N}$, one gets $C = X^T X/(N_r - 1) = \mathrm{diag}(|c_1|^2, |c_2|^2, \ldots, |c_{\mathcal{N}}|^2)$ and the $S_{\rm PCA}$ becomes

$$S_{\rm PCA} = -\sum_j |c_j|^2 \ln|c_j|^2, \tag{5}$$

which is exactly the definition of the participation entropy. However, let us observe that the correspondence we show is only true in the limiting case $N_r \gg \mathcal{N}$ and that the data set contains exponentially large vectors. Therefore, one could ask if working with different choices of encoding and at finite sampling could provide estimates on the critical parameters of the transition as well.

We show that this is valid by studying the behavior of $S^{\infty}_{\rm PCA} = -\ln\lambda_1$. The rationale behind this is that λ_1 contains all the information needed for spotting the localization transition. In fact, in the localized phase we expect a single wave-function coefficient c_x to be dominant. The sampled data

set should be such that the first explained variance ratio λ_1 is much larger than all the others, namely, there should be a single predominant direction in the data space manifold. On the other hand, in the ergodic regime, all wave-function components should be of the same order, and thus the principal components of the samplings should have all the same importance. There should not be a preferred direction in data space, and the explained variance ratios should vanish with the system size (since the normalization $\sum_j \lambda_j = 1$ is enforced).

In the remainder of the article, we showcase these predictions by exploiting the Anderson model on RRGs. We find that with an appropriate analysis, it is possible to retrieve remarkably good estimations on the position of the critical point of the disordered induced transition and perform a clean finite-size scaling. We do so by employing a modest number of measurements and obtain results that are in agreement with the literature and with statistical errors that are compatible with state-of-the-art methods.

III. MODEL AND RESULTS

Let us consider the Anderson model for a single quantum particle on a random regular graph (RRG). The Hamiltonian of the model is [34]

$$H = -\sum_{\langle x,y\rangle} (|x\rangle\langle y| + |y\rangle\langle x|) + \sum_x \epsilon_x |x\rangle\langle x|, \qquad (6)$$

where x, y are integers that label the node of the graph. The Hamiltonian consists of two terms. The first one is the adjacency matrix of the graph ($\langle x, y\rangle$ denotes nearest-neighbor sites), in which, by construction, each node (or vertex) has connectivity K_0 (i.e., fixed vertex degree $\mathcal{D} = K_0 + 1$). The second term represents a random field applied on each site, with the parameters ϵ_i being independent and identically distributed random variables sampled according to the box distribution $g(\epsilon) = \theta(|\epsilon| - W/2)/W$. Denoting with $\mathcal{N}$ the number of vertices of the graph, we introduce a length scale $L = \ln_{K_0} \mathcal{N}$, representing the diameter of the graph, i.e., the maximal length of the shortest paths connecting two nodes.

For $K_0 = 2$, which will be assumed in the rest of the paper, the critical value of the disorder is known to be $W_c \simeq 18.17$ [12,39,42,47]. For $W \ll W_c$ the system is ergodic, and spectral quantities in the thermodynamic limit assume the values predicted by random matrix theory. By increasing W at finite system size, the model displays a crossover to the localized regime, where Poisson statistics describes the energy spectrum. Such a crossover becomes a phase transition in the thermodynamic limit, with the crossover point drifting to larger W as $\mathcal{N}$ is increased and reaching W_c in the $\mathcal{N} \to \infty$ limit [12,13,42]. To find the critical disorder for which the whole system ceases to be ergodic, one has to focus on eigenstates near the middle of the spectrum, i.e., around zero energy for the model under consideration. This is because the eigenstates in the middle of the spectrum are those that need more disorder to localize [48,49] (on the contrary, the ground state is always localized).

The numerical simulations on the model in Eq. (6) are performed as follows. To find the eigenstates, we execute a full exact diagonalization of its matrix for $L \leqslant 14$, or employ the POLFED algorithm for larger system sizes [50]. We calculate $\sim\sqrt{\mathcal{N}}$ eigenvectors in the middle of the spectrum. For each one (see Fig. 1), (1) we sample, according to the probabilities $|c_x|^2$, the corresponding basis vectors $|\psi_x\rangle$. Since the problem is single-particle, we consider the basis $|\psi_x\rangle = |x\rangle$ where the particle occupies the site x. Then, the output of a single sampling will be the position of the particle x. (2) We encode the information as a L-dimensional vector corresponding to the binary representation of the integer x; (3) we perform the analysis on the data set, and (4) average the results over a number of realizations of the disordered Hamiltonian in Eq. (6) ranging from $O(10^4)$ for the smallest sizes to $O(10^2)$ for $L = 17$.

We look at the behavior of $S^{\infty}_{\mathrm{PCA}}$ as a function of the strength of the disorder W and for different sizes of the graph, that we distinguish via the lengthscale L [see Fig. 1(d)]. We observe that $S^{\infty}_{\mathrm{PCA}} = -\ln\lambda_1$ shows a crossover from the delocalized to the localized phase. In the limit of infinite disorder, the wave function is fully localized and it is expected that $S^{\infty}_{\mathrm{PCA}}$ approaches 0. On the other side, in the limiting case $W \sim 0$, there is no preferential configuration sampled. All the nonvanishing λ_j are the same, and thus $\lambda_1 \sim 1/L$. This holds for any $W < W_c$ in the large L limit. We show the behavior of λ_1 for $W = 1$ in Fig. 2(c), as a function of $1/L$, observing that it displays the expected behavior for large L.

To estimate the critical point W_c, we study the intersection of $S^{\infty}_{\mathrm{PCA}}$ with the horizontal line $S^{\infty}_{\mathrm{PCA}} = 1$ since the position of the intersection point W^* drifts when increasing the size of the graph, approaching eventually W_c. Different choices of the position of the line give results compatible with the ones shown here. We plot the behavior of W^* as a function of $1/L$ in Fig. 2(a). Here we report the results in the case $N_r = \sqrt{\mathcal{N}}$ (orange), $N_r = \mathcal{N}/4$ (purple), and $N_r = 5\mathcal{N}$ (black) and we perform a parabolic fit in $1/L$ to estimate W_c. We observe that both extrapolations give a value that is compatible with the one in the literature, also in the case of a modest number of configurations sampled. In particular, we find $W_c(\sqrt{\mathcal{N}}) = 17.78 \pm 0.23$, $W_c(\mathcal{N}/4) = 18.04 \pm 0.36$ and $W_c(5\mathcal{N}) = 18.53 \pm 0.26$, where the critical value of the disorder is $W_c = 18.17 \pm 0.01$. Let us remark here that the critical value $W_c = 18.17 \pm 0.01$ is obtained by solving self-consistent equations for the propagator on the Bethe lattice [47], thus allowing for a higher precision. Instead, state-of-the-art numerical methods to estimate W_c on RRGs have errors on the estimates that are compatible with the ones of our approach [12,42].

To address the critical exponents, we perform a finite-size scaling of $S^{\infty}_{\mathrm{PCA}}$. We employ the scaling ansatz presented in Ref. [12] for the average gap ratio, which in our case takes the form

$$S^{\infty}_{\mathrm{PCA}} = f[(W - W_c)L^{1/\nu}] + L^{-\omega} f_1[(W - W_c)L^{1/\nu}], \qquad (7)$$

where $f(x)$ and f_1 are, respectively, the leading and subleading scaling functions and ν and ω are the critical exponents. Here, ν governs the divergence of the correlation length at the critical point when $W \to W_c^-$ and does not depend on the specific observable. In Ref. [12] it was found to be $\nu = 1$. On the other hand, ω governs the behavior of the observable under analysis at the critical point $W = W_c$. In the case of the

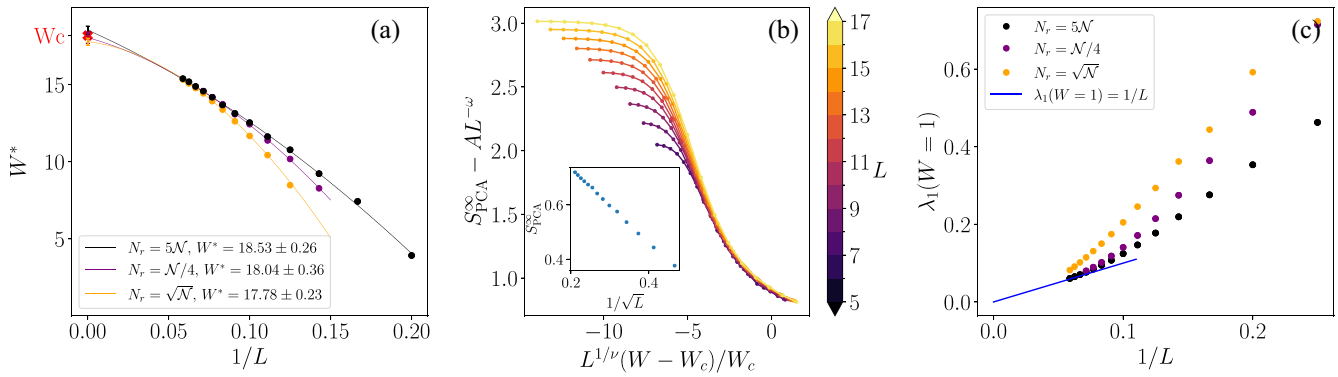

FIG. 2. (a) Plot of W^* versus $1/L$. The extrapolation to $L \to \infty$ gives the correct position of the critical point $W_c = 18.17$, denoted with a red cross. Three different sets of points are shown: black dots obtained by sampling the eigenstates $N_r = 5\mathcal{N}$ times; purple points employing $N_r = \mathcal{N}/4$ samples; and orange dots using $N_r = \sqrt{\mathcal{N}}$. A parabolic fit in $1/L$, the easiest curve accounting for the curvature of the points, is performed and the critical value of W is extrapolated at $1/L = 0$. The fitting functions are $W^* = 18.53 \pm 0.26 + (-46.73 \pm 4.66)/L + (-128.27 \pm 18.57)/L^2$ (black), $W^* = 18.04 \pm 0.36 + (-29.31 \pm 7.01)/L + (-272.44 \pm 32.85)/L^2$ (purple), and $W^* = 17.78 \pm 0.23 + (-13.45 \pm 5.40)/L + (-475.69 \pm 31.19)/L^2$ (orange). In Ref. [43] we elaborate more on the fitting procedure. (b) Plot of the finite-size scaling of $S^{\infty}_{\mathrm{PCA}}$ [as in Eq. (7)]. We fix $\nu = 1$ and $\omega = 1/2$ (according to the result shown in the inset), we use the value of W_c independently obtained in panel (a) and only tune the parameter A to obtain the collapse. The plot of $S^{\infty}_{\mathrm{PCA}} = -\log \lambda_1$ is reported in Fig. 1(d). Notice that we focus on $W < W_c$ as we are interested in the critical exponents when approaching the critical point from the delocalized side. [(b), inset] Behavior of $S^{\infty}_{\mathrm{PCA}}$ at $W = W_c$ as a function of $L^{-1/2}$; we observe $S^{\infty}_{\mathrm{PCA}} \sim L^{-\omega}$ with $\omega = 1/2$. (c) Behavior of $\lambda(W = 1)$ versus $1/L$, both for $N_r = 5\mathcal{N}$ (black) and $N_r = \mathcal{N}/4$ (orange) samples. It is expected, at large sizes, that λ_1 in the ergodic phase goes as $1/L$, being the inverse of the rank of the matrix C. This behavior is indeed reached at large sizes as all sets of points approach the $1/L$ line in blue, which is a guide for the eye.

average gap ratio, it is found $\omega = 2$ [12]. In our case, we find $\omega = 1/2$ for $S^{\infty}_{\mathrm{PCA}}$, as it can be seen from the inset of Fig. 2(b). Setting $\nu = 1$ we obtain a very clean collapse in Fig. 2(b). We approximated the subleading scaling function $f_1(x)$ with a constant A, which is the only free parameter of our analysis, and we set $W_c = 18.17$ [12,39,42,47], as we found above in Fig. 2(a).

IV. CONCLUSION AND OUTLOOK

In this article, we introduced a nonparametric unsupervised learning approach to tackle localization transitions. We connected analytically the eigendecomposition of the sample covariance matrix to the participation entropy, physically motivating our approach. We showcased it on the Anderson model on a random regular graph that, even if noninteracting, displays important features that are reminiscent of many-body localization and presents a serious challenge both analytically and numerically. Exploiting this example we showed that disordered quantum systems can be characterized with data-science-inspired approaches and localization transitions can also be seen as geometric transitions in data space.

We studied the infinite order Rényi entropy $S^{\infty}_{\mathrm{PCA}}$ of the eigenvalues covariance matrix as a function of disorder strength and system size to extract an estimate of the critical value of the disorder W_c, that is remarkably in agreement with results in the literature — in particular, considering the hard challenge presented by the model investigated [12,42]. As observed in Fig. 2(a), a modest number of measurements suffices for estimating the transition point, such that the approach described here can be considered of practical use for nowadays quantum simulators with local addressing.

Furthermore, we performed a finite-size scaling of $S^{\infty}_{\mathrm{PCA}}$ by employing the scaling ansatz presented in Ref. [12] for the average gap ratio, and we obtained results compatible with the literature.

We observe that the method employed requires no *a priori* knowledge of the physical system under investigation, being then a powerful tool also in the study of other physical scenarios, in particular, many-body problems. We present results for the "Imbrie model" [51,52], in the Supplemental Material [43] (see also Refs. [53–55] therein). It is believed to display many-body localization, and thus we exploit it to prove that our method is applicable also to interacting scenarios.

We note that the same analysis could be performed to tackle problems such as out-of-equilibrium phase transitions or the classification of quantum phases of matter. Moreover, one could try to understand if this kind of approach could be used in combination with randomized measurements [56,57], to extract relevant features of many-body quantum states prepared in the laboratory.

ACKNOWLEDGMENTS

The authors acknowledge M. Dalmonte, C. Muzzi, R. V. Aranda, and A. Scardicchio for useful discussions, and F. Balducci, G. Chiriacò, A. Gambassi, P. Sierant, and X. Turkeshi for comments on the manuscript. V.V. is grateful to X. Turkeshi for useful insights and for drawing his attention to the participation entropy. C.V. thanks P. Sierant for sharing the POLFED code that was used in this work for the numerical simulations at large system sizes. Work in Grenoble was funded by the French National Research Agency via QUBITAF (ANR-22-PETQ-0004, Plan France 2030).

[1] M. Rigol, V. Dunjko, and M. Olshanii, Thermalization and its mechanism for generic isolated quantum systems, Nature (London) **452**, 854 (2008).

[2] A. Polkovnikov, K. Sengupta, A. Silva, and M. Vengalattore, *Colloquium*: Nonequilibrium dynamics of closed interacting quantum systems, Rev. Mod. Phys. **83**, 863 (2011).

[3] D. A. Abanin, E. Altman, I. Bloch, and M. Serbyn, *Colloquium:* Many-body localization, thermalization, and entanglement, Rev. Mod. Phys. **91**, 021001 (2019).

[4] J. Smith, A. Lee, P. Richerme, B. Neyenhuis, P. W. Hess, P. Hauke, M. Heyl, D. A. Huse, and C. Monroe, Many-body localization in a quantum simulator with programmable random disorder, Nat. Phys. **12**, 907 (2016).

[5] M. Schreiber, S. S. Hodgman, P. Bordia, H. P. Lüschen, M. H. Fischer, R. Vosk, E. Altman, U. Schneider, and I. Bloch, Observation of many-body localization of interacting fermions in a quasirandom optical lattice, Science **349**, 842 (2015).

[6] O. Shtanko, D. S. Wang, H. Zhang, N. Harle, A. Seif, R. Movassagh, and Z. Minev, Uncovering local integrability in quantum many-body dynamics, arXiv:2307.07552.

[7] D. H. White, T. A. Haase, D. J. Brown, M. D. Hoogerland, M. S. Najafabadi, J. L. Helm, C. Gies, D. Schumayer, and D. A. Hutchinson, Observation of two-dimensional Anderson localisation of ultracold atoms, Nat. Commun. **11**, 4942 (2020).

[8] J. Billy, V. Josse, Z. Zuo, A. Bernard, B. Hambrecht, P. Lugan, D. Clément, L. Sanchez-Palencia, P. Bouyer, and A. Aspect, Direct observation of Anderson localization of matter waves in a controlled disorder, Nature (London) **453**, 891 (2008).

[9] G. Roati, C. D'Errico, L. Fallani, M. Fattori, C. Fort, M. Zaccanti, G. Modugno, M. Modugno, and M. Inguscio, Anderson localization of a non-interacting Bose–Einstein condensate, Nature (London) **453**, 895 (2008).

[10] S. Wold, K. Esbensen, and P. Geladi, Principal component analysis, Chemom. Intell. Lab. Syst. **2**, 37 (1987).

[11] I. T. Jolliffe, *Principal Component Analysis for Special Types of Data* (Springer, New York, 2002).

[12] P. Sierant, M. Lewenstein, and A. Scardicchio, Universality in Anderson localization on random graphs with varying connectivity, SciPost Phys. **15**, 045 (2023).

[13] C. Vanoni, B. L. Altshuler, V. E. Kravtsov, and A. Scardicchio, Renormalization group analysis of the Anderson model on random regular graphs, arXiv:2306.14965.

[14] A. Kutlin and C. Vanoni, Investigating finite-size effects in random matrices by counting resonances, arXiv:2402.10271.

[15] J. Šuntajs, M. Hopjan, W. D. Roeck, and L. Vidmar, Similarity between a many-body quantum avalanche model and the ultrametric random matrix model, Phys. Rev. Res. **6**, 023030 (2024).

[16] P. Kunkel, M. Prüfer, S. Lannig, R. Rosa-Medina, A. Bonnin, M. Gärttner, H. Strobel, and M. K. Oberthaler, Simultaneous readout of noncommuting collective spin observables beyond the standard quantum limit, Phys. Rev. Lett. **123**, 063603 (2019).

[17] T. Brydges, A. Elben, P. Jurcevic, B. Vermersch, C. Maier, B. P. Lanyon, P. Zoller, R. Blatt, and C. F. Roos, Probing Rényi entanglement entropy via randomized measurements, Science **364**, 260 (2019).

[18] J. C. Hoke, M. Ippoliti, D. Abanin, R. Acharya, M. Ansmann, F. Arute, K. Arya, A. Asfaw, J. Atalaya, J. C. Bardin *et al.*, Quantum information phases in space-time: measurement-induced entanglement and teleportation on a noisy quantum processor, Nature (London) **622**, 481 (2023).

[19] V. Vitale, A. Rath, P. Jurcevic, A. Elben, C. Branciard, and B. Vermersch, Estimation of the quantum Fisher information on a quantum processor, arXiv:2307.16882.

[20] J. Carrasquilla and R. G. Melko, Machine learning phases of matter, Nat. Phys. **13**, 431 (2017).

[21] S. J. Wetzel, Unsupervised learning of phase transitions: From principal component analysis to variational autoencoders, Phys. Rev. E **96**, 022140 (2017).

[22] T. Mendes-Santos, X. Turkeshi, M. Dalmonte, and A. Rodriguez, Unsupervised learning universal critical behavior via the intrinsic dimension, Phys. Rev. X **11**, 011040 (2021).

[23] T. Mendes-Santos, A. Angelone, A. Rodriguez, R. Fazio, and M. Dalmonte, Intrinsic dimension of path integrals: Data-mining quantum criticality and emergent simplicity, PRX Quantum **2**, 030332 (2021).

[24] X. Turkeshi, Measurement-induced criticality as a data-structure transition, Phys. Rev. B **106**, 144313 (2022).

[25] R. K. Panda, R. Verdel, A. Rodriguez, H. Sun, G. Bianconi, and M. Dalmonte, Non-parametric learning critical behavior in Ising partition functions: PCA entropy and intrinsic dimension, SciPost Phys. Core **6**, 086 (2023).

[26] V. Vitale, T. Mendes-Santos, A. Rodriguez, and M. Dalmonte, Topological Kolmogorov complexity and the Berezinskii-Kosterlitz-Thouless mechanism, Phys. Rev. E **109**, 034102 (2024).

[27] R. Verdel, V. Vitale, R. K. Panda, E. D. Donkor, A. Rodriguez, S. Lannig, Y. Deller, H. Strobel, M. K. Oberthaler, and M. Dalmonte, Data-driven discovery of statistically relevant information in quantum simulators, Phys. Rev. B **109**, 075152 (2024).

[28] T. Mendes-Santos, M. Schmitt, A. Angelone, A. Rodriguez, P. Scholl, H. J. Williams, D. Barredo, T. Lahaye, A. Browaeys, M. Heyl, and M. Dalmonte, Wave function network description and Kolmogorov complexity of quantum many-body systems, Phys. Rev. X **14**, 021029 (2024).

[29] L. Wang, Discovering phase transitions with unsupervised learning, Phys. Rev. B **94**, 195105 (2016).

[30] W. Hu, R. R. P. Singh, and R. T. Scalettar, Discovering phases, phase transitions, and crossovers through unsupervised machine learning: A critical examination, Phys. Rev. E **95**, 062122 (2017).

[31] S. Bradde and W. Bialek, PCA meets RG, J. Stat. Phys. **167**, 462 (2017).

[32] P. Mehta, M. Bukov, C.-H. Wang, A. G. Day, C. Richardson, C. K. Fisher, and D. J. Schwab, A high-bias, low-variance introduction to machine learning for physicists, Phys. Rep. **810**, 1 (2019).

[33] J. Carrasquilla, Machine learning for quantum matter, Adv. Phys.: X **5**, 1797528 (2020).

[34] P. W. Anderson, Absence of diffusion in certain random lattices, Phys. Rev. **109**, 1492 (1958).

[35] K. Tikhonov and A. Mirlin, From Anderson localization on random regular graphs to many-body localization, Ann. Phys. **435**, 168525 (2021).

[36] K. S. Tikhonov, A. D. Mirlin, and M. A. Skvortsov, Anderson localization and ergodicity on random regular graphs, Phys. Rev. B **94**, 220203(R) (2016).

[37] V. Kravtsov, B. Altshuler, and L. Ioffe, Non-ergodic delocalized phase in Anderson model on bethe lattice and regular graph, Ann. Phys. (NY) **389**, 148 (2018).

[38] A. De Luca, B. L. Altshuler, V. E. Kravtsov, and A. Scardicchio, Anderson localization on the bethe lattice: Nonergodicity of extended states, Phys. Rev. Lett. **113**, 046806 (2014).

[39] G. Parisi, S. Pascazio, F. Pietracaprina, V. Ros, and A. Scardicchio, Anderson transition on the bethe lattice: An approach with real energies, J. Phys. A: Math. Theor. **53**, 014003 (2020).

[40] G. De Tomasi, S. Bera, A. Scardicchio, and I. M. Khaymovich, Subdiffusion in the Anderson model on the random regular graph, Phys. Rev. B **101**, 100201(R) (2020).

[41] S. Bera, G. De Tomasi, I. M. Khaymovich, and A. Scardicchio, Return probability for the Anderson model on the random regular graph, Phys. Rev. B **98**, 134205 (2018).

[42] M. Pino, Scaling up the Anderson transition in random-regular graphs, Phys. Rev. Res. **2**, 042031(R) (2020).

[43] See Supplemental Material at http://link.aps.org/supplemental/10.1103/PhysRevB.110.024204 for more details and our analysis.

[44] B. L. Altshuler, V. E. Kravtsov, A. Scardicchio, P. Sierant, and C. Vanoni, Renormalization group for Anderson localization on high-dimensional lattices, arXiv:2403.01974.

[45] A. Kutlin and I. M. Khaymovich, Anatomy of the eigenstates distribution: a quest for a genuine multifractality, SciPost Phys. **16**, 008 (2024).

[46] P. Sierant and X. Turkeshi, Universal behavior beyond multifractality of wave functions at measurement-induced phase transitions, Phys. Rev. Lett. **128**, 130605 (2022).

[47] K. S. Tikhonov and A. D. Mirlin, Critical behavior at the localization transition on random regular graphs, Phys. Rev. B **99**, 214202 (2019).

[48] N. Mott, The mobility edge since 1967, J. Phys. C: Solid State Phys. **20**, 3075 (1987).

[49] B. A. Van Tiggelen, Localization of waves, Diffuse waves in complex media **531**, 1 (1999).

[50] P. Sierant, M. Lewenstein, and J. Zakrzewski, Polynomially filtered exact diagonalization approach to many-body localization, Phys. Rev. Lett. **125**, 156601 (2020).

[51] J. Z. Imbrie, On many-body localization for quantum spin chains, J. Stat. Phys. **163**, 998 (2016).

[52] D. Abanin, J. Bardarson, G. De Tomasi, S. Gopalakrishnan, V. Khemani, S. Parameswaran, F. Pollmann, A. Potter, M. Serbyn, and R. Vasseur, Distinguishing localization from chaos: Challenges in finite-size systems, Ann. Phys. (NY) **427**, 168415 (2021).

[53] A. Morningstar, L. Colmenarez, V. Khemani, D. J. Luitz, and D. A. Huse, Avalanches and many-body resonances in many-body localized systems, Phys. Rev. B **105**, 174205 (2022).

[54] D. J. Luitz, F. Huveneers, and W. De Roeck, How a small quantum bath can thermalize long localized chains, Phys. Rev. Lett. **119**, 150602 (2017).

[55] W. De Roeck and F. Huveneers, Stability and instability towards delocalization in many-body localization systems, Phys. Rev. B **95**, 155129 (2017).

[56] A. Elben, S. T. Flammia, H.-Y. Huang, R. Kueng, J. Preskill, B. Vermersch, and P. Zoller, The randomized measurement toolbox, Nat. Rev. Phys. **5**, 9 (2023).

[57] P. Cieśliński, S. Imai, J. Dziewior, O. Gühne, L. Knips, W. Laskowski, J. Meinecke, T. Paterek, and T. Vértesi, Analysing quantum systems with randomised measurements, arXiv:2307.01251.